DIFFRACTION OF LIMIT PERIODIC POINT SETS

MICHAEL BAAKE AND UWE GRIMM

Abstract. Limit periodic point sets are aperiodic structures with pure point diffraction supported on a countably, but not finitely generated Fourier module that is based on a lattice and certain integer multiples of it. Examples are cut and project sets with p-adic internal spaces. We illustrate this by explicit results for the diffraction measures of two examples with 2-adic internal spaces. The first and well-known example is the period doubling sequence in one dimension, which is based on the period doubling substitution rule. The second example is a weighted planar point set that is derived from the classic chair tiling in the plane. It can be described as a fixed point of a block substitution rule.

1. Introduction

The diffraction measure is a characteristic property of a translation bounded measure ω on Euclidean space (or on any locally compact Abelian group) and has important applications in crystallography because it describes the outcome of kinematic diffraction (from X-rays or neutron scattering, say). It is the Fourier transform $\widehat{\gamma}$ of the autocorrelation measure γ of ω. Following the discovery of quasicrystals (which are generally non-periodic but nevertheless show pure point or Bragg diffraction), measures with pure point diffraction have been investigated thoroughly. In parallel, there has also been progress in understanding singular continuous and absolutely continuous diffraction; see [3, 4] and references therein. Let us mention in passing that making a connection with the spectra of Schrödinger operators is tempting, but has so far eluded all attempts to substantiate it.

In this article, within the realm of pure point diffractive systems, we consider two examples of limit periodic structures, the period doubling sequence in one dimension (Section 3) and point sets related to the chair tiling in two dimensions (Section 4). The corresponding point sets arise from fixed points of (block) substitution rules, but also have a description as cut and project sets with 2-adic internal spaces. We begin with a concise survey of the relevant quantities, where we restrict ourselves to measures that are supported on integer lattices. Then, the two main examples are presented in an informal way, though all results are rigorous (with the underlying mathematical framework being available via [11, 7, 6]). A more detailed exposition will appear in [5].

2. Autocorrelation and diffraction of Dirac combs

Consider the (weighted) Dirac comb $\omega = \sum_{x\in\mathbb{Z}^d} w(x)\delta_x$, with δ_x the normalised point (or Dirac) measure at $x \in \mathbb{Z}^d$ and (in general, complex) weights

$w(x)$. The *natural autocorrelation* (if it exists) of ω is defined as the Eberlein convolution

$$\gamma \,=\, \omega \circledast \widetilde{\omega} \,:=\, \lim_{N\to\infty} \frac{\omega_N * \widetilde{\omega_N}}{\mathrm{vol}\bigl([-N,N]^d\bigr)}, \tag{1}$$

which we view as a measure on $\mathbb{R}^d$. Here, $\omega_N = \omega|_{[-N,N]^d}$ denotes the restriction of ω to the closed cube $[-N,N]^d$, and $\widetilde{\mu}$ is the 'flipped over' measure, defined by $\widetilde{\mu}(g) = \overline{\mu(\widetilde{g})}$ with g a continuous test function of compact support and $\widetilde{g}(x) = \overline{g(-x)}$, the bar denoting complex conjugation. In all cases considered below, the limit in (1) exists. Due to $\mathrm{supp}(\omega) \subset \mathbb{Z}^d$, the autocorrelation is then of the form

$$\gamma \,=\, \sum_{z\in\mathbb{Z}^d} \eta(z)\, \delta_z \tag{2}$$

with the autocorrelation coefficients

$$\eta(z) \,=\, \lim_{N\to\infty} \frac{1}{(2N+1)^d} \sum_{x\in\mathbb{Z}^d\cap[-N,N]^d} w(x)\, \overline{w(x-z)}. \tag{3}$$

The existence of the limit in (1) is equivalent to the existence of the autocorrelation coefficients $\eta(z)$ for all $z \in \mathbb{Z}^d$.

By construction, γ is a positive definite measure, and its Fourier transform $\widehat{\gamma}$ thus exists. The latter is a positive, translation bounded measure on $\mathbb{R}^d$ (by the Bochner-Schwartz theorem), which is known as the *diffraction measure* of ω. It corresponds to the (kinematic) diffraction from the measure ω; compare [8] for background and [11, 6] for this approach to diffraction theory. The diffraction measure possesses the unique decomposition

$$\widehat{\gamma} = \bigl(\widehat{\gamma}\bigr)_{\mathsf{pp}} + \bigl(\widehat{\gamma}\bigr)_{\mathsf{sc}} + \bigl(\widehat{\gamma}\bigr)_{\mathsf{ac}} \tag{4}$$

into its pure point, singular continuous and absolutely continuous parts, the latter splitting relative to Lebesgue measure, the natural reference measure for volume in Euclidean space. Lattice periodic measures in $\mathbb{R}^d$ give rise to pure point diffraction, as do regular model sets with Euclidean internal space $\mathbb{R}^m$, where the diffraction measure is supported on a $\mathbb{Z}$-module of finite rank $m+d$; see [6] and references therein for more. The examples discussed below are also based on model sets, but with 2-adic internal spaces; they are *limit periodic*, and thus exhibit pure point diffraction where the corresponding Fourier module is countably, but not finitely generated. For both examples, the explicit form of the diffraction can be obtained either from the cut and project description [6] or from the inflation structure [10]; in this note, we use the latter approach.

3. The period doubling sequence

The *period doubling sequence* is defined by the primitive substitution rule

$$\varrho : \begin{array}{l} a \mapsto ab \\ b \mapsto aa \end{array} \tag{5}$$

on the two-letter alphabet $\{a, b\}$. It is related to the classic Thue-Morse system (as a factor under a $2:1$ mapping; compare [3] and references therein) and

defines a strictly ergodic dynamical system via the orbit closure of a suitable bi-infinite sequence. The latter can be obtained from a fixed point of ϱ^2 via the iteration

$$a|a \xrightarrow{\varrho^2} abaa|abaa \xrightarrow{\varrho^2} \dots \longrightarrow w = \varrho^2(w), \tag{6}$$

with convergence in the (obvious) product topology. Here, $|$ marks the origin of a two-sided sequence $w = \dots w_{-2}w_{-1}|w_0w_1\dots$, and we start with the legal seed $a|a$. The half-infinite word $v = w_0w_1\dots$ is the (unique) one-sided fixed point of ϱ.

To the sequence w, we associate two point sets $\varLambda_\ell \subset \mathbb{Z}$ with $\ell \in \{a,b\}$ via

$$\varLambda_\ell = \{n \in \mathbb{Z} \mid w_n = \ell\},$$

so $\varLambda_a \dot\cup \varLambda_b = \mathbb{Z}$, where $\dot\cup$ denotes the disjoint union of sets. The geometric fixed point equation for ϱ^2 now implies the equations

$$\varLambda_a = 4\varLambda_a \,\dot\cup\, (4\varLambda_a + 2) \,\dot\cup\, (4\varLambda_a + 3) \,\dot\cup\, 4\varLambda_b \,\dot\cup\, (4\varLambda_b + 2), \tag{7a}$$

$$\varLambda_b = (4\varLambda_a + 1) \,\dot\cup\, (4\varLambda_b + 1) \,\dot\cup\, (4\varLambda_b + 3), \tag{7b}$$

which can be decoupled and solved by iteration, yielding

$$\varLambda_a = \{-1\} \,\dot\cup\, \dot{\bigcup_{i\geq 0}}\bigl(2\cdot 4^i\mathbb{Z} + (4^i - 1)\bigr), \quad \varLambda_b = \dot{\bigcup_{i\geq 1}}\bigl(4^i\mathbb{Z} + (2\cdot 4^{i-1} - 1)\bigr), \tag{8}$$

where the singleton set $\{-1\}$ has to be added to the fixed point (to either $\varLambda_a$ or $\varLambda_b$), as it is only a limit point under 2-adic completion [7].

We attach a Dirac comb to $\varLambda_\ell$ by $\omega_\ell := \delta_{\varLambda_\ell} = \sum_{n\in\varLambda_\ell} \delta_n$ for $\ell \in \{a,b\}$. A general weighted Dirac comb with weights α (for letter a) and β (for letter b) can then be expressed as $\omega = \alpha\omega_a + \beta\omega_b$. Its autocorrelation measure exists and has the form of Eq. (2) (with $d = 1$) with autocorrelation coefficients $\eta(z)$ according to (3), where the weight $w(x) \in \{\alpha,\beta\}$ is chosen according to the letter at position $x \in \mathbb{Z}$.

For simplicity, we work with the one-sided fixed point v (which has the same autocorrelation). We first consider weights $\alpha = 1$ and $\beta = -1$, and denote the autocorrelation coefficients for this balanced case by $\eta_\pm(z)$. The corresponding sequence $\{v_i\}_{i\in\mathbb{N}_0}$ of weights $v_i \in \{\pm 1\}$ satisfies the recursions $v_{2n} = 1$ and $v_{2n+1} = -v_n$ for $n \geq 0$. This implies a recursion for the autocorrelation coefficients,

$$\eta_\pm(2m) = \frac{1}{2}\bigl(1 + \eta_\pm(m)\bigr) \quad \text{and} \quad \eta_\pm(2m+1) = -\frac{1}{3}, \tag{9}$$

for all $m \geq 0$. In particular, $\eta_\pm(0) = 1$, and we also have $\eta_\pm(-m) = \eta_\pm(m)$. When $m = 2^r(2s+1)$ with $r, s \geq 0$, the recursion leads to

$$\eta_\pm(m) = 1 - \frac{1}{3\cdot 2^{r-2}},$$

which is independent of s. Going back to general weights α and β amounts to considering the bi-infinite sequence $\frac{1}{2}\bigl((\alpha+\beta)\mathbf{1} + (\alpha-\beta)w\bigr)$, or alternatively $\frac{1}{2}\bigl((\alpha+\beta)\mathbf{1} + (\alpha-\beta)v\bigr)$ for its one-sided counterpart, which results in

$$\eta \;=\; \tfrac{1}{4}(\alpha-\beta)^2\eta_\pm + \tfrac{1}{12}\bigl(3(\alpha+\beta)^2 + 2(\alpha^2-\beta^2)\bigr)\mathbf{1}. \tag{10}$$

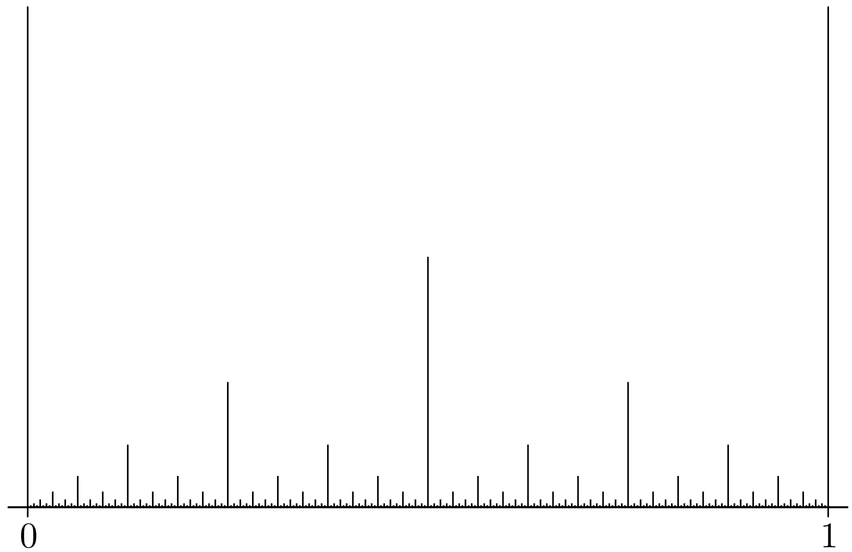

FIGURE 1. Sketch of the diffraction amplitudes $|A(k)|$ from Eq. (12) for the period doubling chain, with $k \in [0,1]$. The diffraction pattern repeats $\mathbb{Z}$-periodically along the real line [2].

Taking the Fourier transform, the diffraction measure is obtained as

$$\widehat{\gamma} \,=\, \sum_{k\in L^{\circledast}} \bigl|\alpha A(k) + \beta B(k)\bigr|^2 \,\delta_k, \tag{11}$$

where $L^{\circledast} = \bigcup_{s\geq 1} \mathbb{Z}/2^s = \bigl\{ \frac{m}{2^r} \mid (r = 0,\, m \in \mathbb{Z}) \text{ or } (r \geq 1,\, m \text{ odd})\bigr\}$ is the *Fourier module* of the period doubling sequence. The amplitudes read

$$A(k) = \frac{2}{3\cdot(-2)^r}\, e^{2\pi i k} \quad \text{and} \quad B(k) = \delta_{r,0} - A(k), \tag{12}$$

where we implicitly refer to the parametrisation of $L^{\circledast}$.

To derive these formulas, one observes that a finite union in Eq. (8) would still be a periodic set, whose diffraction can be calculated by direct Fourier transform (which is then a periodic point measure) followed by taking the absolute square of the amplitudes (note that the Wiener diagram is still commutative in this case). This results in a sequence of pure point measures that converge not only in the vague topology, but also in the stronger norm topology towards the diffraction measure in (11), with the amplitudes as in (12); see [6] for details. Since pure point measures are closed in the norm topology, this also gives the constructive proof that $L^{\circledast}$ is indeed the Fourier module.

As mentioned above, the same result can also be derived via the description of the periodic doubling sequence as a model set with 2-adic internal space; see [7, 6] for a proof. A sketch of the diffraction pattern is shown in Figure 1.

The presence of the powers of 2^{-s} in the Fourier module shows the limit periodic structure; since s can be arbitrarily large, the Fourier module cannot be finitely generated. Nevertheless, the diffraction measure is pure point, with

amplitudes that reflect the inflation symmetry with integer multiplier 2, as visible in Figure 1.

4. Block substitution for the chair tiling

Let us move on to our planar example. Consider the block substitution rule

$$0 \mapsto \begin{array}{cc} 1 & 0 \\ 0 & 3 \end{array} \qquad 1 \mapsto \begin{array}{cc} 1 & 2 \\ 0 & 1 \end{array} \qquad 2 \mapsto \begin{array}{cc} 1 & 2 \\ 2 & 3 \end{array} \qquad 3 \mapsto \begin{array}{cc} 3 & 2 \\ 0 & 3 \end{array} \tag{13}$$

on the alphabet $\{0,1,2,3\}$. Iterating the rule, starting from a legal seed,

$$\begin{array}{c|c} 3 & 0 \\ \hline 2 & 1 \end{array} \;\longmapsto\; \begin{array}{cc|cc} 3 & 2 & 1 & 0 \\ 0 & 3 & 0 & 3 \\ \hline 1 & 2 & 1 & 2 \\ 2 & 3 & 0 & 1 \end{array} \;\longmapsto\; \begin{array}{cccc|cccc} 3 & 2 & 1 & 2 & 1 & 2 & 1 & 0 \\ 0 & 3 & 2 & 3 & 0 & 1 & 0 & 3 \\ 1 & 0 & 3 & 2 & 1 & 0 & 3 & 2 \\ 0 & 3 & 0 & 3 & 0 & 3 & 0 & 3 \\ \hline 1 & 2 & 1 & 2 & 1 & 2 & 1 & 2 \\ 0 & 1 & 2 & 3 & 0 & 1 & 2 & 3 \\ 1 & 2 & 3 & 2 & 1 & 0 & 1 & 2 \\ 2 & 3 & 0 & 3 & 0 & 3 & 0 & 1 \end{array} \;\longmapsto\; \cdots \tag{14}$$

produces a sequence of growing square-shaped blocks (with lines denoting the coordinate axes, so the origin is located in the centre of the blocks), where each block reappears in the centre of the next. This sequence thus converges in the product topology, where the limit is a fixed point of the block substitution rule that covers the entire square lattice. This fixed point has a D_4 colour symmetry: An anti-clockwise rotation through $\pi/2$ corresponds to the cyclic permutation (0123), while a reflection in the central horizontal gives the permutation $(01)(23)$. The pattern is thus invariant under any D_4 transformation followed by an appropriate permutation.

If we choose a representation with four different unit squares and take the lower left corners as their reference points, the fixed point defined by (14) results in a partition $\mathbb{Z}^2 = \varLambda_0 \dot\cup \varLambda_1 \dot\cup \varLambda_2 \dot\cup \varLambda_3$ of $\mathbb{Z}^2$ into four point sets of equal density $\frac{1}{4}$. As a result of (13), they satisfy the fixed point equations

$$\varLambda_0 = 2\varLambda_0 \,\dot\cup\, (2\varLambda_0 + u + v) \,\dot\cup\, 2\varLambda_1 \,\dot\cup\, 2\varLambda_3, \tag{15a}$$

$$\varLambda_1 = (2\varLambda_0 + v) \,\dot\cup\, (2\varLambda_1 + u) \,\dot\cup\, (2\varLambda_1 + v) \,\dot\cup\, (2\varLambda_2 + v), \tag{15b}$$

$$\varLambda_2 = (2\varLambda_1 + u + v) \,\dot\cup\, 2\varLambda_2 \,\dot\cup\, (2\varLambda_2 + u + v) \,\dot\cup\, (2\varLambda_3 + u + v), \tag{15c}$$

$$\varLambda_3 = (2\varLambda_0 + u) \,\dot\cup\, (2\varLambda_2 + u) \,\dot\cup\, (2\varLambda_3 + u) \,\dot\cup\, (2\varLambda_3 + v), \tag{15d}$$

with $u = (1,0)^T$ and $v = (0,1)^T$. Denoting the even and odd sublattices of $\mathbb{Z}^2$ as $\varGamma_+ = \big\{(x_1,x_2)^T \in \mathbb{Z}^2 \;\big|\; x_1 + x_2 \equiv 0 \bmod 2\big\}$ and $\varGamma_- = u + \varGamma_+$, we have $\mathbb{Z}^2 = \varGamma_+ \dot\cup \varGamma_-$, as well as $\varLambda_0 \dot\cup \varLambda_2 = \varGamma_+$ and $\varLambda_1 \dot\cup \varLambda_3 = \varGamma_-$. This leads to the decoupled equations

$$\varLambda_0 = 2\varGamma_- \,\dot\cup\, \big(2\varLambda_0 + \{0, u+v\}\big) \quad \text{and} \quad \varLambda_1 = \big(2\varGamma_+ + v\big) \,\dot\cup\, \big(2\varLambda_1 + \{u,v\}\big), \tag{16}$$

together with $\varLambda_2 = \varGamma_+ \setminus \varLambda_0$ and $\varLambda_3 = \varGamma_- \setminus \varLambda_1$. An explicit solution is (with $Sx := \{sx \mid s \in S\}$ for sets $S \subset \mathbb{Z}$ and $S_r := \{0, 1, \dots, 2^r - 1\}$ for $r \geq 0$)

$$\varLambda_0 = \mathbb{N}_0(u+v) \,\dot{\cup} \dot{\bigcup}_{r\geq 0} \big(2^{r+1}\varGamma_- + S_r(u+v)\big), \tag{17a}$$

$$\varLambda_1 + v = \mathbb{N}_0(u-v) \,\dot{\cup} \dot{\bigcup}_{r\geq 0} \big(2^{r+1}\varGamma_- + S_r(u-v)\big), \tag{17b}$$

$$\varLambda_2 + u + v = -\mathbb{N}_0(u+v) \,\dot{\cup} \dot{\bigcup}_{r\geq 0} \big(2^{r+1}\varGamma_- - S_r(u+v)\big), \tag{17c}$$

$$\varLambda_3 + u = -\mathbb{N}_0(u-v) \,\dot{\cup} \dot{\bigcup}_{r\geq 0} \big(2^{r+1}\varGamma_- - S_r(u-v)\big), \tag{17d}$$

where we used $\varGamma_+ + u = \varGamma_+ + v = \varGamma_- = \varGamma_- + u + v$. Each of the infinite unions on the right-hand side defines a point set of density $\frac{1}{4}$. The sets of points (of density 0) along the diagonals have to be added for our fixed point (14), because they are not contained in any of the lattice translates (but are covered by the 2-adic completion of the infinite unions, similar to the situation of the period doubling sequence). The solutions obey the relations $\varLambda_0 \dot{\cup} \varLambda_2 = \varGamma_+$ and $\varLambda_1 \dot{\cup} \varLambda_3 = \varGamma_-$.

Now, we are going to calculate the diffraction measure of the Dirac comb

$$\omega = \sum_{i=0}^{3} \alpha_i \, \delta_{\varLambda_i} \tag{18}$$

with the four point sets $\varLambda_i$ from Eq. (17), and arbitrary complex numbers α_i.

Define $Q_r(x) := 2^{r+1}\varGamma_- + S_r x$ for $r \in \mathbb{N}_0$ and $x \in \mathbb{Z}^2$. Using $\varGamma_+^* = \frac{1}{2}\varGamma_+$ (where the superscript $*$ denotes the dual lattice), we calculate

$$\begin{aligned} \widehat{\delta_{Q_r(x)}} &= \sum_{m=0}^{2^r-1} \mathrm{e}^{-2\pi\mathrm{i}mkx} \big(\delta_{2^{r+1}(\varGamma_+ + u)}\big)^{\widehat{}} = \frac{1-\mathrm{e}^{-2^{r+1}\pi\mathrm{i}kx}}{1-\mathrm{e}^{-2\pi\mathrm{i}kx}} \, \mathrm{e}^{-2^{r+2}\pi\mathrm{i}ku} \, \widehat{\delta_{2^{r+1}\varGamma_+}} \\ &= \frac{1-\mathrm{e}^{-2^{r+1}\pi\mathrm{i}kx}}{1-\mathrm{e}^{-2\pi\mathrm{i}kx}} \, \frac{\mathrm{e}^{-2^{r+2}\pi\mathrm{i}ku}}{2^{2r+3}} \, \delta_{\varGamma_+/2^{r+2}}, \end{aligned} \tag{19}$$

where we again write density factors as functions of k. The first fraction evaluates as 2^r whenever $kx \in \mathbb{Z}$ (by an application of the l'Hospital rule). The resulting Fourier module is

$$L^{\circledast} = \bigcup_{s\geq 2} \frac{\varGamma_+}{2^s} = \mathbb{Z}^2 \,\dot{\cup} \dot{\bigcup}_{s\geq 1} \Big\{ \frac{1}{2^s}(m,n) \mid m,n \in \mathbb{Z} \text{ with } \gcd(m,n,2) = 1 \Big\}, \tag{20}$$

which is the coarsest group that contains all positions where the Fourier transform in (19) has a point measure.

The diffraction measure of our weighted Dirac comb ω is of the form

$$\widehat{\gamma_\omega} = \sum_{k \in L^{\circledast}} \Big| \sum_{i=0}^{3} \alpha_i \, A_i(k) \Big|^2 \delta_k, \tag{21}$$

where $A_i(k)$ is the amplitude that belongs to $\varLambda_i$. Its derivation is analogous to the method explained above for the period doubling sequence (via periodic

approximants that converge in the norm topology). This method also provides a proof for the correctness of (20).

The amplitudes themselves can be calculated in the same way as for the period doubling sequence above. For any $k \in L^{\circledast}$, there is a minimal $s \geq 0$ such that $k \in \varGamma_+/2^{s+2}$, and then $k \in \varGamma_+/2^{r+2}$ for all $r \geq s$. The amplitudes result from summing the corresponding contributions from Eq. (19), with $x = u + v$ for $i = 0$, $x = u - v$ for $i = 1$, $x = -u - v$ for $i = 2$ and $x = -u + v$ for $i = 3$. In addition, the results have to be multiplied by an overall phase factor that reflects the translation vectors on the left-hand sides of the four relations in Eq. (17). We omit the detailed (and somewhat lengthy) calculations and simply state the result.

To this end, the integer and half-integer points of $L^{\circledast}$ are better treated separately. Whenever $k \in \mathbb{Z}^2$,

$$A_0(k) = A_1(k) = A_2(k) = A_3(k) = \frac{1}{4}. \tag{22}$$

If $k \in \frac{1}{2}\varGamma_+ \setminus \mathbb{Z}^2$, one has $k = \frac{1}{2}(m,n)$ with m and n odd, so that $kx \in \mathbb{Z}$ for all $x \in \varGamma_+$. This gives

$$A_0(k) = A_2(k) = \frac{1}{4} \quad \text{and} \quad A_1(k) = A_3(k) = -\frac{1}{4}, \tag{23}$$

while $k = \frac{1}{2}(m,n)$ with $m + n$ odd results in

$$A_0(k) = \frac{1}{8}, \quad A_2(k) = -\frac{1}{8}, \quad A_1(k) = \frac{(-1)^n}{8} \quad \text{and} \quad A_3(k) = \frac{(-1)^m}{8}. \tag{24}$$

In particular, $A_0(k) + A_2(k) = 0$, and also $A_1(k) + A_3(k) = 0$, as $m + n$ is odd.

The remaining elements of $L^{\circledast}$ are of the form $k = (m,n)/2^s$ with $s \geq 2$ and $m, n \in \mathbb{Z}$ subject to the condition $\gcd(m,n,2) = 1$. The amplitudes $A_0(k)$ and $A_2(k)$ depend on $m + n$. They satisfy $A_2(k) = -A_0(k)$ and

$$A_0(k) = \begin{cases} 0, & \text{if } 2^s \mid (m+n), \\ -\dfrac{2}{4^s}\,\dfrac{1-(-1)^{(m+n)/2}}{1-\varepsilon_s^{m+n}}, & \text{if } m+n \text{ even with } 2^s \nmid (m+n), \\ \dfrac{1}{4^s}\,\dfrac{1}{1-\varepsilon_s^{m+n}}, & \text{if } m+n \text{ odd,} \end{cases} \tag{25}$$

where $\varepsilon_s = \exp(-2\pi\mathrm{i}/2^s)$ is a root of unity. Similarly, one obtains the relation $A_3(k) = -A_1(k)$ together with

$$A_1(k) = \varepsilon_s^{-n} \begin{cases} 0, & \text{if } 2^s \mid (m-n), \\ -\dfrac{2}{4^s}\,\dfrac{1-(-1)^{(m-n)/2}}{1-\varepsilon_s^{m-n}}, & \text{if } m-n \text{ even with } 2^s \nmid (m-n), \\ \dfrac{1}{4^s}\,\dfrac{1}{1-\varepsilon_s^{m-n}}, & \text{if } m-n \text{ odd.} \end{cases} \tag{26}$$

In particular, $\alpha_0 = \alpha_1 = \alpha_2 = \alpha_3 = 1$ leads to $\widehat{\gamma_\omega} = \delta_{\mathbb{Z}^2}$, as required. Moreover, setting $\alpha_0 = \alpha_2 = 1$ and $\alpha_1 = \alpha_3 = 0$ gives the diffraction $\widehat{\gamma_\omega} = \widehat{\delta_{\varGamma_+}} = \frac{1}{2}\delta_{\varGamma_+/2}$, while the alternative choice $\alpha_0 = \alpha_2 = 0$ together with $\alpha_1 = \alpha_3 = 1$ yields (using the parametrisation of k as above) $\widehat{\gamma_\omega} = \widehat{\delta_{\varGamma_-}} = \mathrm{e}^{-2\pi\mathrm{i}ku}\,\widehat{\delta_{\varGamma_+}} = \frac{(-1)^m}{2}\,\delta_{\varGamma_+/2}$.

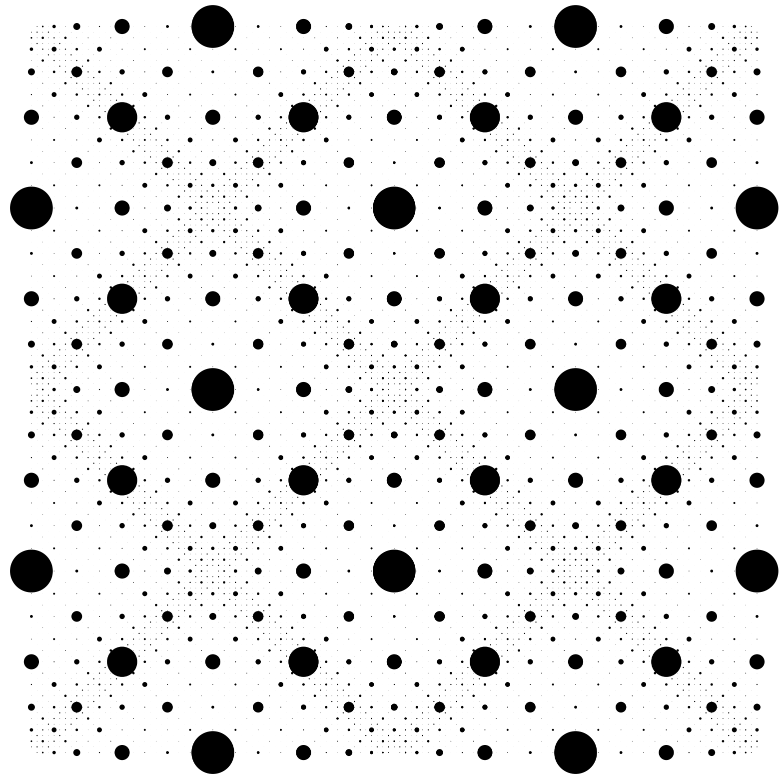

FIGURE 2. Illustration of the diffraction measure for the Dirac comb (21) with weights $\alpha_j = \mathrm{i}^j$, where $j \in \{0,1,2,3\}$. A peak at $k \in [-1,1]^2$ is represented by a black disc, centred at k, with an area proportional to the peak intensity. The complete pattern is $\frac{1}{2}\varGamma_{+}$-periodic.

An interesting case results from the balanced choice $\alpha_j = \mathrm{i}^j$, which produces extinctions for all $k \in \frac{1}{2}\varGamma_{+}$. The corresponding diffraction measure is illustrated in Figure 2. It is D_4-symmetric, which is not the case in general.

For a generic choice of the weights, our Dirac comb (18) is mutually locally derivable (MLD) with the chair tiling. As it is based on four subsets of $\mathbb{Z}^2$, the diffraction measure $\widehat{\gamma_\omega}$ is always $\mathbb{Z}^2$-periodic [2]. This is the generic maximal translation symmetry. However, since $\varLambda_0 \dot\cup \varLambda_2 = \varGamma_{+}$, the diffraction of any weighted Dirac comb with only these two components is periodic under the dual lattice $\varGamma_{+}^{*} = \frac{1}{2}\varGamma_{+}$. Likewise, the corresponding statement holds for the diffraction of weighted Dirac combs with components $\varLambda_1$ and $\varLambda_3$. This is also the translation symmetry in Figure 2, which is a consequence of the particular choice of the weights here.

Any choice of the weights refers to a discrete structure that can be viewed as a decoration of the chair tiling, and is thus locally derivable from it. Conversely, a typical decoration of the chair tiling will be locally derivable from our coloured

point set, but need not be realisable as a simple decoration of the square-shaped building blocks. In this sense, our above results constitute only a first step of the complete diffraction analysis of the chair tiling.

5. Summary and Outlook

Limit periodic structures form an interesting class of pure point diffractive systems. Explicit results for the diffraction can be obtained, at least for examples such as those discussed in this paper; related examples can be found in [1, 13].

Limit periodic tilings also arise in the context of Wang tiles. Raphael Robinson's tilings consisting of six square-shaped prototiles [14], up to rotations and reflections, is one example. In this case, the limit periodic structure is apparent from a hierarchical pattern of interlocking squares of larger and larger sizes. Recently, a similar tiling with a single hexagonal prototile, up to rotations and reflections, was discovered [15, 16], with a hierarchical pattern of interlocking triangles. It is related to the half-hex inflation that was studied in detail in [9], where also its limit-periodic structure was derived, and to Penrose's $(1+\varepsilon+\varepsilon^2)$ tiling [12].

The new example is particularly intriguing because the hexagon is the first example of a single aperiodic tile (provided you count the tile and its mirror image as a single tile), in the sense that there exist local rules that allow the existence of tilings covering the entire plane, but no such tiling can have any non-trivial period. The local rules involve not just neighbours, but also the next corona, and thus cannot be encapsulated in the shape of a tile whose interior is connected; see [15] for details. It would be interesting to study the diffraction properties of these tilings, which will reflect the limit periodic structure apparent in the patterns of squares and triangles.

Acknowledgements

This work was supported by the German Research Council (DFG), within the CRC 701, and by a Leverhulme Trust Visiting Professorship Grant (MB).

References

[1] J.-P. Allouche and M. Mendez-France, Automata and automatic sequences, in: *Beyond Quasicrystals*, F. Axel and D. Gratias, eds., Springer, Berlin, 1995, pp. 293–367.

[2] M. Baake, Diffraction of weighted lattice subsets, Can. Math. Bulletin 45 (2002) pp. 483–498.

[3] M. Baake and U. Grimm, The singular continuous diffraction measure of the Thue-Morse chain, J. Phys. A: Math. Theor. 41 (2008) 422001.

[4] M. Baake and U. Grimm, Kinematic diffraction is insufficient to distinguish order from disorder, Phys. Rev. B 79 (2009) 020203(R) and 80 (2009) 029903(E).

[5] M. Baake and U. Grimm, *The Theory of Aperidoic Order – A Mathematical Invitation*, in preparation (to appear with Cambridge University Press).

[6] M. Baake and R.V. Moody, Weighted Dirac combs with pure point diffraction, J. reine angew. Math. (Crelle) 573 (2004) pp. 61–94.

[7] M. Baake, R.V. Moody and M. Schlottmann, Limit-(quasi)periodic point sets as quasicrystals with p-adic internal spaces, J. Phys. A: Math. Gen. 31 (1998) pp. 5755–5765.

[8] J.M. Cowley, *Diffraction Physics*, 3rd edition, North-Holland, Amsterdam, 1995.

[9] D. Frettlöh, *Nichtperiodische Pflasterungen mit ganzzahligem Inflationsfaktor*, PhD thesis, Univ. Dortmund, 2002; available via `http://www.math.uni-bielefeld.de/baake/frettloe/research.html`.

[10] F. Gähler and R. Klitzing, The diffraction pattern of self-similar tilings, in: *The Mathematics of Long-Range Aperiodic Order*, R.V. Moody, ed., NATO ASI C 489, Kluwer, Dordrecht, 1997, pp. 141–174.

[11] A. Hof, On diffraction by aperiodic structures, Commun. Math. Phys. 169 (1995) pp. 25–43.

[12] R. Penrose, Remarks on tiling: Details of a $(1+\varepsilon+\varepsilon^2)$-aperiodic set, in: *The Mathematics of Long-Range Aperiodic Order*, R.V. Moody, ed., NATO ASI C 489, Kluwer, Dordrecht, 1997, pp. 467–497.

[13] M. Queffelec, Spectral study of automatic and substitutive sequences, in: *Beyond Quasicrystals*, F. Axel and D. Gratias, eds., Springer, Berlin, and Les Edition de Physique, Les Ulis, 1995, pp. 369–414.

[14] R.M. Robinson, Undecidability and nonperiodicity for tilings of the plane, Invent. Math. 12 (1971) pp. 177–209.

[15] J.E.S. Socolar and J.M. Taylor, An aperiodic hexagonal tile, preprint arXiv:1003.4279 (2010).

[16] J.M. Taylor, Aperiodicity of a functional monotile, Preprint Bielefeld CRC 701: 0-015 (2010), available via `http://www.math.uni-bielefeld.de/sfb701`.

Fakultät für Mathematik, Universität Bielefeld, Postfach 100131, 33501 Bielefeld, Germany (MB)

Department of Mathematics and Statistics, The Open University, Walton Hall, Milton Keynes MK7 6AA, UK (UG)

School of Mathematics and Physics, University of Tasmania, Private Bag 37, Hobart, Tasmania 7001, Australia (MB and UG)